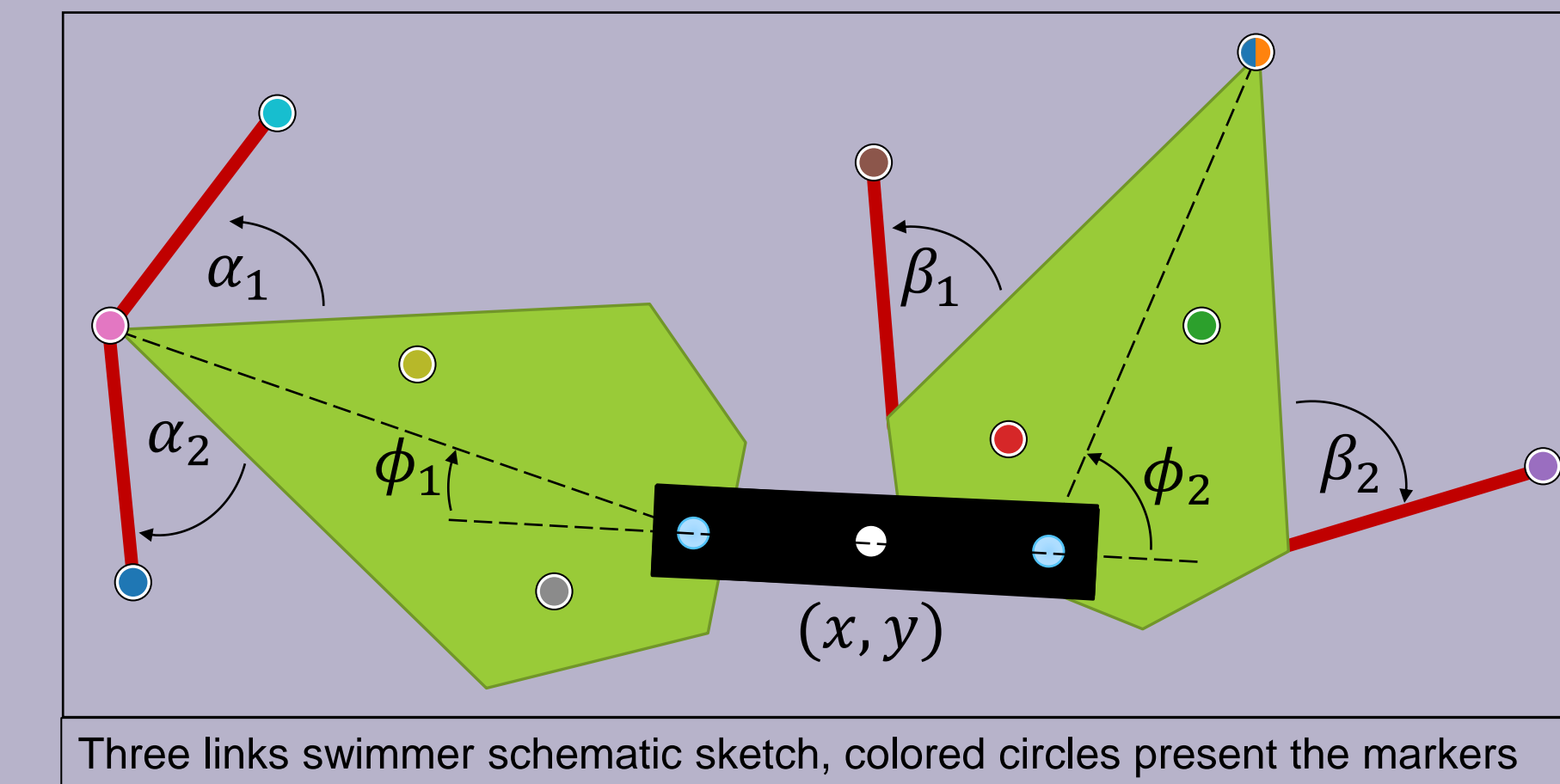


Shape-underactuated systems modeling and control

Zvi Chapnik, Yizhar Or and Shai Revzen

Abstract:

Geometric mechanics provides valuable insights into how biological and robotic systems use changes in shape to move by mechanically interacting with their environment. This perspective produced an approach for obtaining simplified data-driven models for locomotion systems directly from motion tracking data. Here we focus on the locomotion of under-actuated robotic systems with passive shape degrees of freedom (DoF), interacting with a granular fluid - a regime we intentionally selected because it is hard to model. We compared four modeling approaches, predicting body velocity both within gait and across gaits. Switching our model from a phase dependent linear model to a manifold learning approach reduced velocity prediction error by 55% but required 6 times as much data; including the passive DoF in the models reduced prediction errors by 4%. These improvements compound, and yield overall R^2 values above 90%, demonstrating that our data-driven geometric mechanics models for locomotion systems can produce highly predictive models even where no first principles equations of motion are known.



Swimmer properties

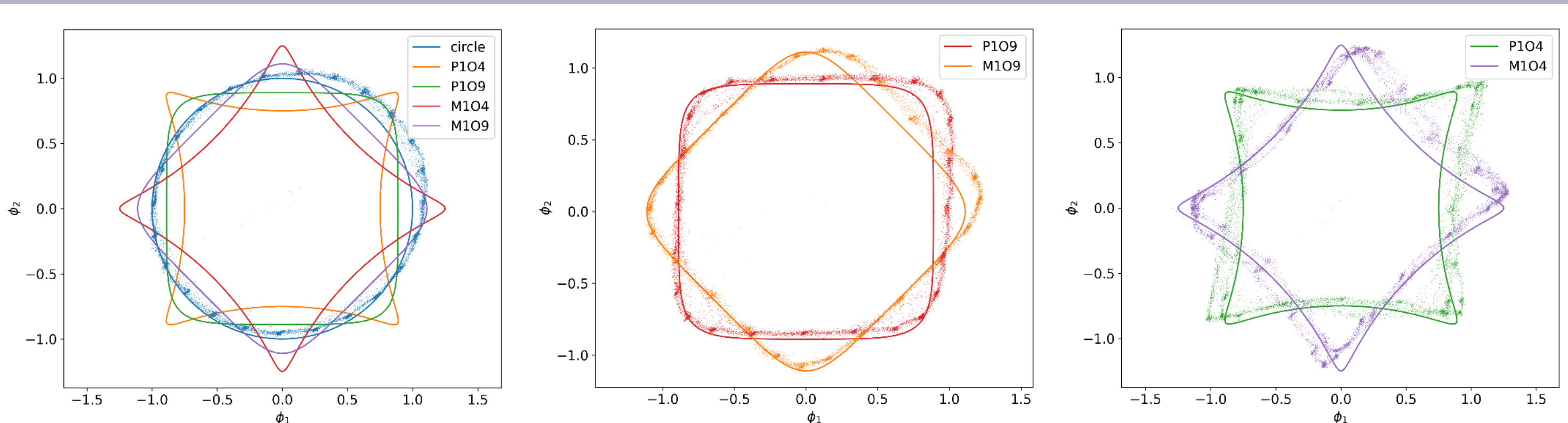
Three links swimmer.
Two actuated angles ϕ_1, ϕ_2 .
Four flippers α_1, α_2 and β_1, β_2 , changing passively with a maximum angle constraint.
Shape variables are $r = [r_a, r_p]$, $r_a = [\phi_1, \phi_2]$, $r_p = [\alpha_1, \alpha_2, \beta_1, \beta_2]$.
Location and orientation are defined by the center of the middle link (x, y) and its orientation angle θ .

Experiments in granular medium-dry beans.

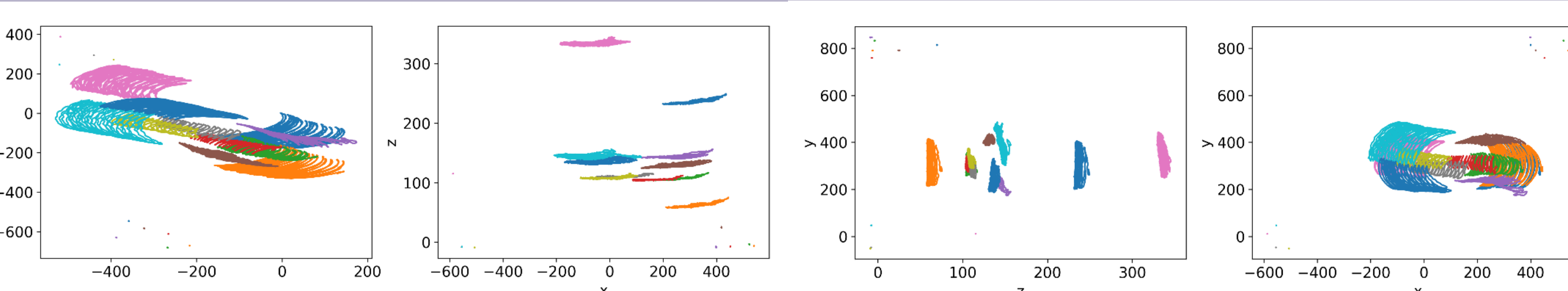


Actuation gaits

Three actuation frequencies (0.33, 0.48, 1) Hz
Five different gait geometries: Circle
the first two components of Fourier's series of a circle:
 $\phi_1 = \cos(\omega t) \mp \cos(3\omega t) / c$
 $\phi_2 = \sin(\omega t) \pm \sin(3\omega t) / c$
 $c = 4, 9$



The different gaits are plotted. On the left figure are all the theoretical gaits and the measured circle gait; on the other two figures, the theoretical and the measured gaits are plotted for the other geometries. The theoretical gaits are represented by solid lines, and actual motion tracking measurements are marked by dots.



The markers measurement from an experiment are plotted in the xy xz zy planes and isometric display are plotted, allowing us to visualize the movement of the swimmer easily. The markers' colors match the colors in the sketch above.

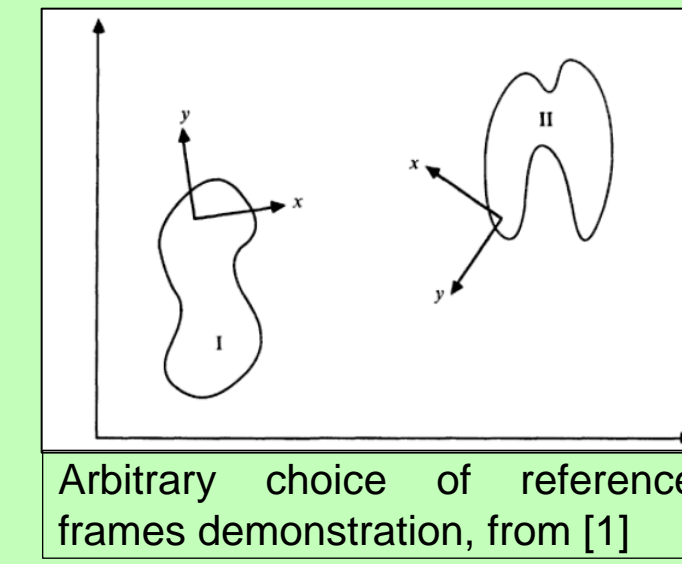
Background

A self-propelled organism or device moves by deforming its shape. These shape changes create stresses in the surrounding fluid, producing the necessary forces and torques for propulsion.

[1,2] Formulate the problem using a geometric approach, introducing the concept of a gauge field on the space of shapes

$$S(t) = \mathfrak{R}(t)S_0(t)$$

$$\mathfrak{R}(t_2) = \mathfrak{R}(t_1)\bar{P}\exp\left[\int_{S_0(t_1)}^{S_0(t_2)} A(S_0)dS_0\right]$$



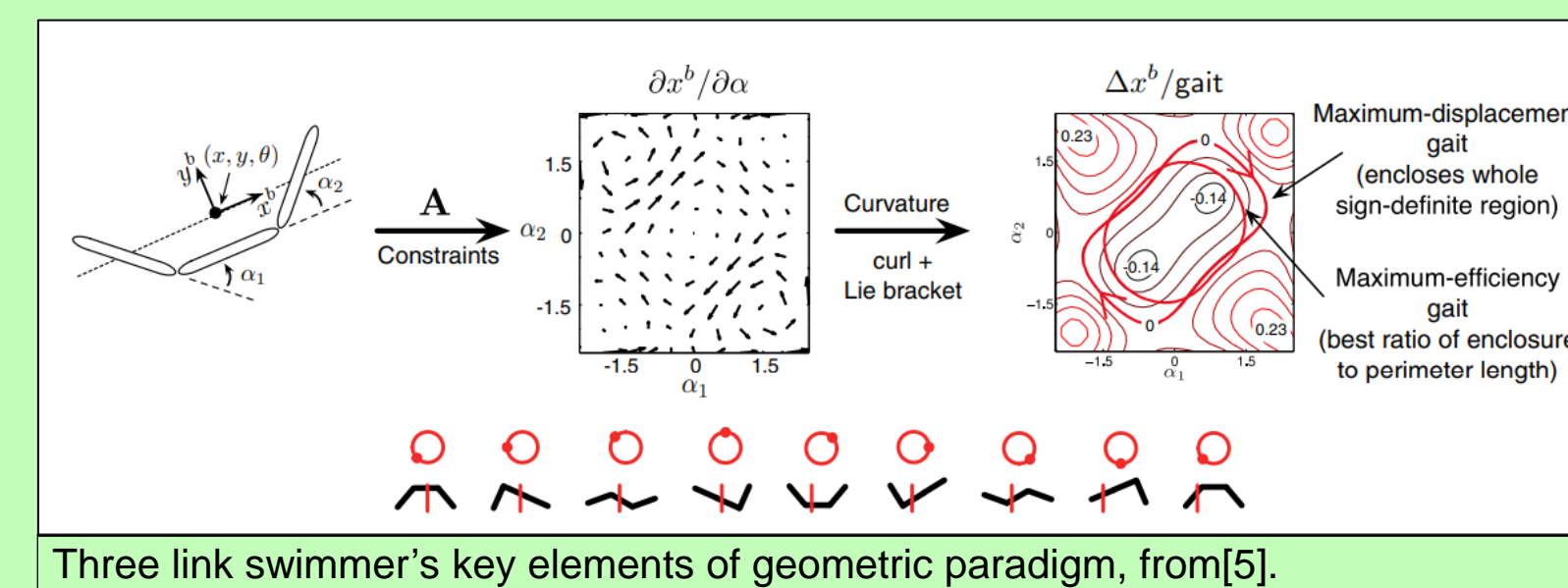
This formulation provides a powerful framework for understanding the mechanics of self-propulsion in viscous environments, where inertial forces are negligible compared to viscous forces.

Geometric Mechanics basic equation:

$$\overset{o}{g} = A(r)\dot{r}$$

Using of gauge structure to model kinematic systems for rhythmic motion-gait.

It is used to optimize gaits and to investigate the kinematic systems [3,4]. The coordinate system chosen is important in order to model the system accurately [5].

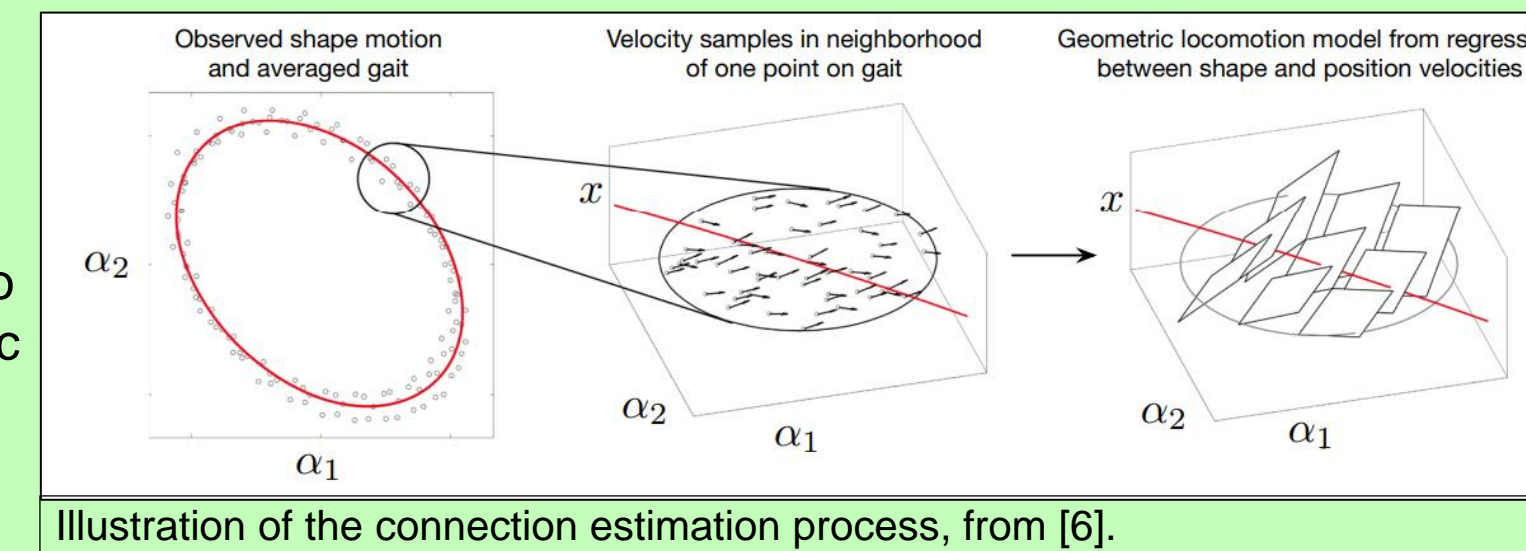


Data-driven Model estimation [6]

Data from real-life systems has noise
Shape vector change from time to phase
The connection matrix has been rewritten for perturbation from the phase-average behavior
From this formulation, we can use total least squares to estimate the connection matrices around specific phase

$$\overset{o}{g}_n^k \sim C^k + B^k \delta_n^j + (A_i^k) \delta_n^i + \left(\frac{\partial A_i^k}{\partial r_j}\right) \delta_n^j \delta_n^i$$

Data size n^2 is needed to evaluate

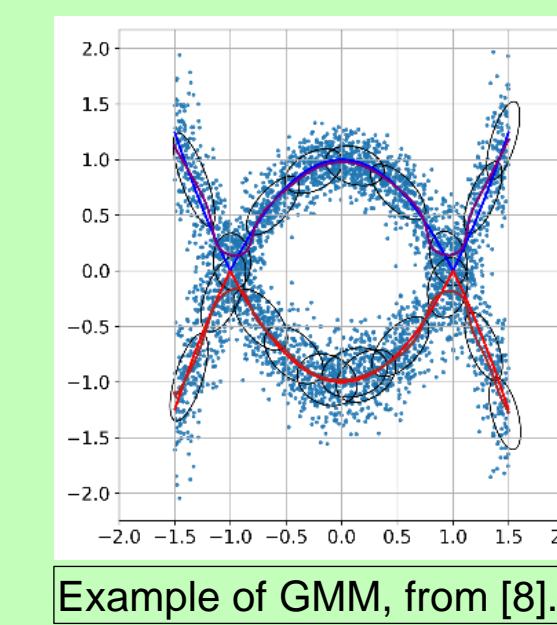


Gaussian mixture model (GMM) [8]

Estimating the connection by the equation $f(v_b, r, \dot{r}) = v_b - A(r)\dot{r} = 0$

Advantages:

- Does not rely on phase estimation, can work with non-periodic motion
- Can handle hysteresis effects
- Nonlinear connection



Geometric mechanics with under-actuated shape variables[7]

Separate the passive part in the connection equation

$$\left(\overset{o}{g}, \dot{r}_p\right)^T = \tilde{C}(r) + B(r)\dot{r}_a$$

Shape vector change from time to phase

The connection matrix has been rewritten for perturbation from the phase-average behavior

From this formulation, we can use total least squares to estimate the connection matrices around specific phase

$$\left(\overset{o}{g}, \dot{r}_p\right)^T \sim C + C_r \delta + B \delta_a + B_r \delta_a$$

Data size nm_a is needed to evaluate

Using GMM to evaluate the connection by this formulation:

$$f(v_b, r, \dot{r}) = \left(\overset{o}{g}, \dot{r}_p\right)^T - \tilde{C}(r) + B(r)\dot{r}_a$$

Results

Actuation in 5 different geometric shapes and three frequencies.

Using each of the gaits to create four geometric mechanics models:

Without passive DoF calculated with total least square(TLS)

With passive DoF calculated with total least square(TLS)

Without passive DoF calculated with Gaussian mixture model (GMM)

With passive DoF calculated with Gaussian mixture model (GMM)

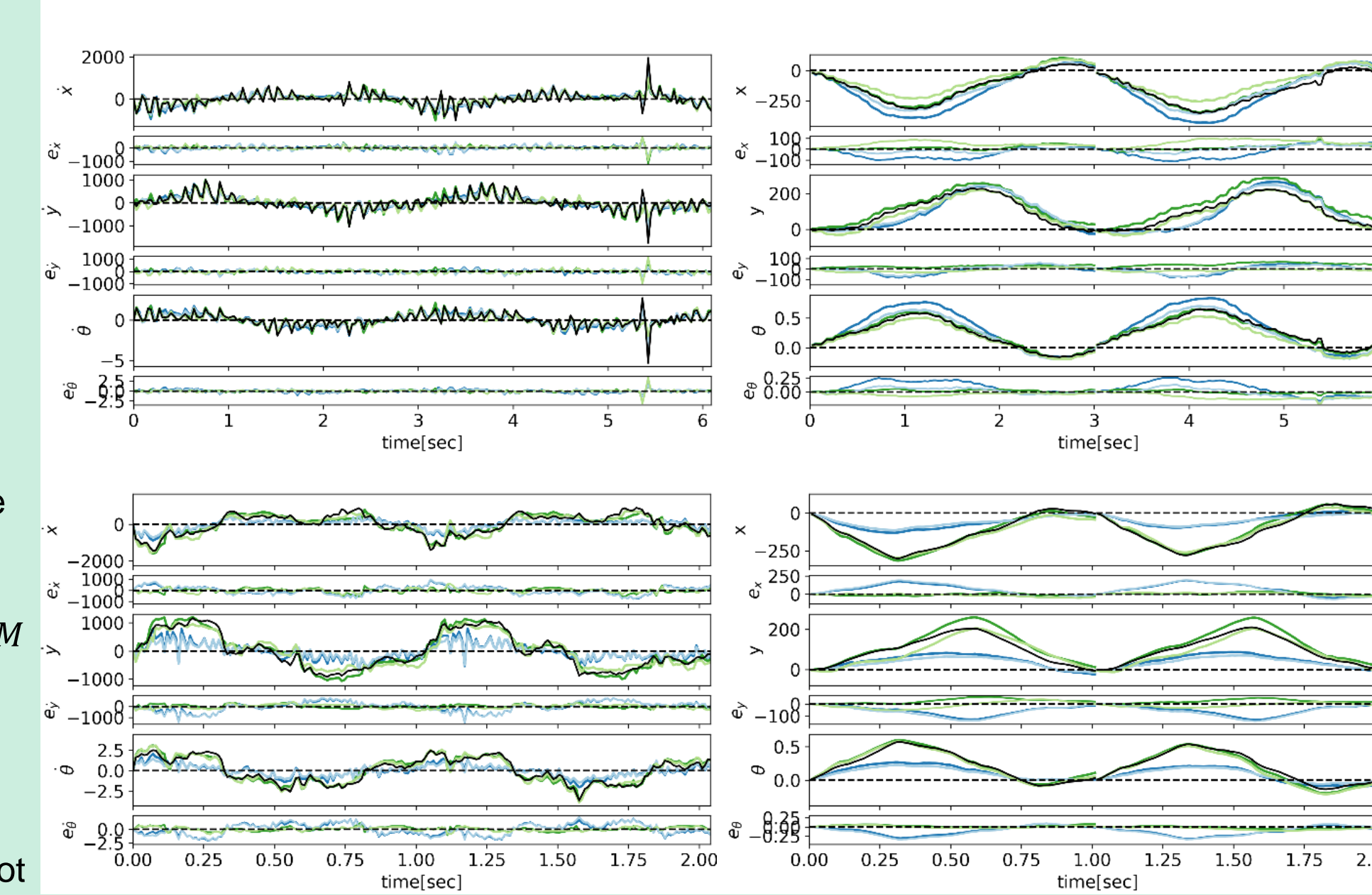
Each of the models is used to estimate all the different gaits

- Ground truth
- no passive DoF TLS
- passive DoF TLS
- no passive DoF GMM
- passive DoF GMM

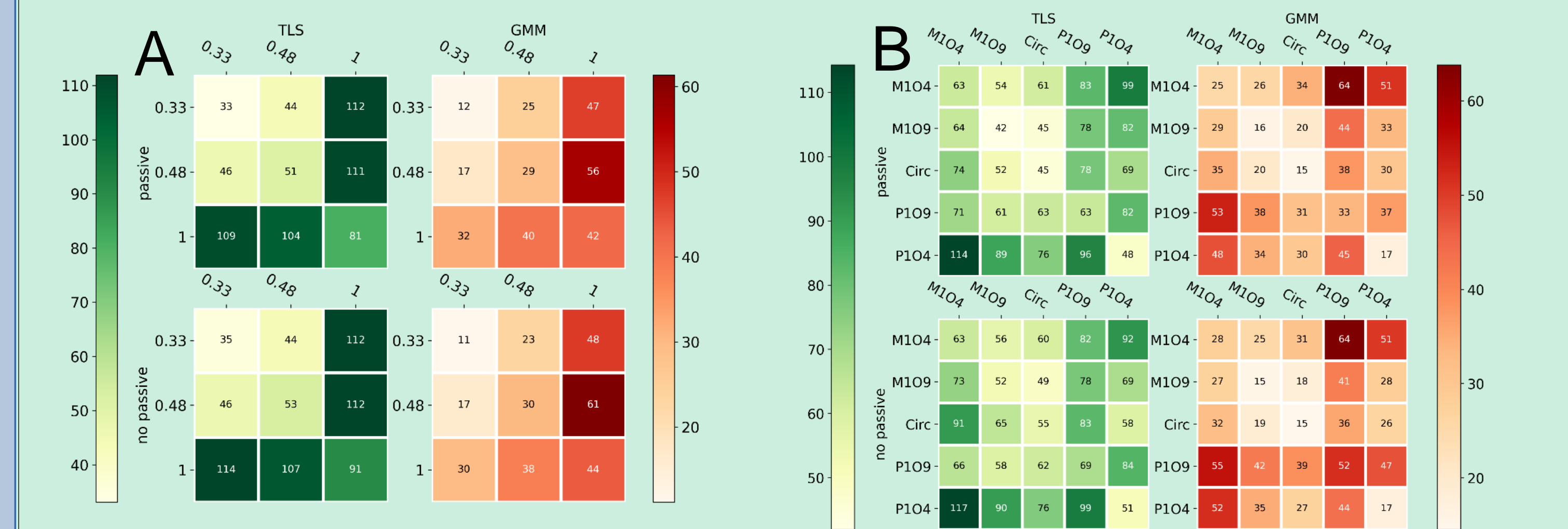
Good prediction for all the models in interpolation (same gait test)

Models with passive DoF get better results- not significant.

In extrapolation, with different geometry and frequency, the different GMM models get better results.



In order to display the results from all of the models and estimations of the different gaits, we present the following heat map plots



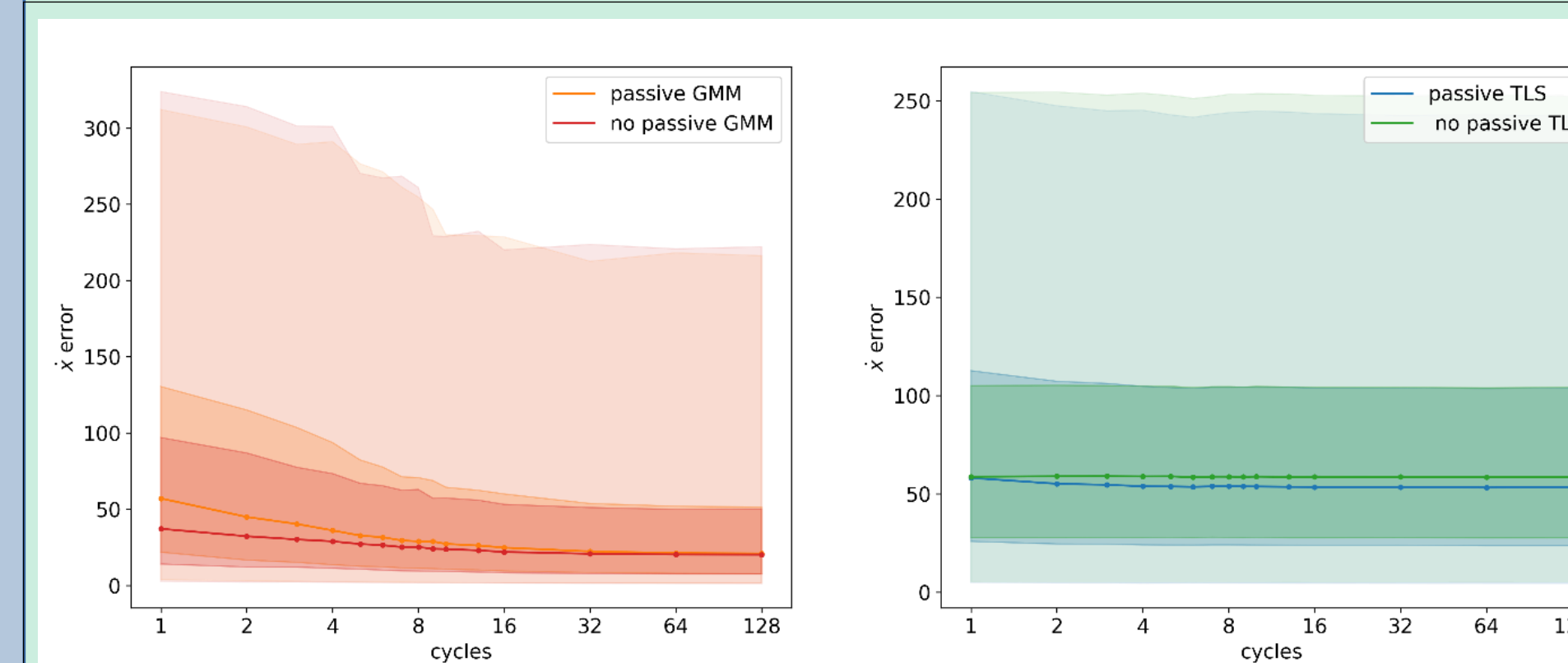
A plot shows the speed error in the x-direction of the estimation for each model at different frequencies. B plot shows the speed error in the x-direction of the estimation for each model in the different gait geometries. Models are in the rows and estimations in the columns. The error was calculated as the percentage of the RMS of the circle 0.48Hz gait speed.

It is easier to estimate the (0.33,0.48) frequencies models.

Geometries- as we move farther away from the diagonal, the estimation becomes poorer

Both of the GMM models get better results than the TLS models.

Models with passive DoF for the TLS calculation get better results- not significant



The plots on the left show the estimation error of the speed in the x-direction from models based on circle, 0.48[Hz] gait as a function of the number of cycles the model is built from.

The results show that the linear models are able to learn the model from around 8 cycles, and the error is constant for any more data used numbers of cycles. For the GMM models, we can see that we need around 60 cycles to learn a good model, from there, there is no significant change in the error.

Discussion and future work

In this work, we presented preliminary results showing that using GM to model robotic systems in granular media is possible; furthermore, the GMM models demonstrated good prediction for nearby gaits. Using that method, we can model a system in a granular medium without adding new features to the model. We also demonstrated that these models were capable of learning from a small dataset. Those results are preliminary, we have more analysis to conduct on this data, and a change of coordinate system to an optimal one is needed [5]. We would like to integrate linear elastic effects into those models and incorporate a non-smooth effect (like the stoppers). We would like to perform new experiments on other robotics systems with more significant influence of their underactuated shape variables.

[1] Shapere, A. and Wilczek, F., 1989. Geometry of self-propulsion at low Reynolds number. *Journal of Fluid Mechanics*, 198, pp.557-585.

[2] Shapere, A. and Wilczek, F., 1989. Gauge kinematics of deformable bodies. *Am. J. Phys.* 57(6), pp.514-518.

[3] Kelly, S.D. and Murray, R.M., 1995. Geometric phases and robotic locomotion. *Journal of Robotic Systems*, 12(6), pp.417-431.

[4] Bloch, A.M., Krishnaprasad, P.S., Marsden, J.E. and Murray, R.M., 1996. Nonholonomic mechanical systems with symmetry. *Archive for rational mechanics and analysis*, 136, pp.21-99.

[5] Hatton, R.L. and Choset, H., 2011. Geometric motion planning: The local connection, Stokes' theorem, and the importance of coordinate choice. *The International Journal of Robotics Research*, 30(8), pp.988-1014.

[6] Bittner, B., Hatton, R.L. and Revzen, S., 2018. Geometrically optimal gaits: a data-driven approach. *Nonlinear Dynamics*, 94(3), pp.1933-1948.

[7] Bittner, B., Hatton, R.L. and Revzen, S., 2022. Data-driven geometric system identification for shape-underactuated dissipative systems. *Bioinspiration & biomimetics*, 17(2), p.026004.

[8] Hu, R. and Revzen, S., 2025. Learning the Geometric Mechanics of Robot Motion Using Gaussian Mixtures. *arXiv preprint arXiv:2502.05309*.